

NONDETERMINISTIC DEFORMATION ANALYSIS USING QUASICONFORMAL GEOMETRY

Han Zhang, Lok Ming Lui

Department of Mathematics
The Chinese University of Hong Kong

ABSTRACT

Deformation analysis is crucial in many applications, especially in medical image analysis. Analyzing the deformation pattern of anatomical structures provides important information for disease analysis. With degraded images or uncertainties, getting a deterministic solution of the deformation is challenging. In some cases, there may also be multiple solutions with different probabilities. As such, it is important to analyze the probability distribution of deformations, given data information with uncertainty. In this work, we propose to use computational Quasiconformal (QC) Teichmüller theories to parameterize the space of deformations. A distribution over the space of special features, called the *QC features*, can be computed and applied for deformation analysis. Extensive experiments are carried out on both synthetic data and real medical images, which demonstrate the efficacy of the proposed framework.

Index Terms— Non-deterministic, deformation analysis, conformal structure, quasiconformal, medical image analysis

1. INTRODUCTION

Medical image analysis is a crucial procedure for disease analysis and disease diagnosis. To analyze anatomical structures captured in medical images, their shape information has to be studied. On the other hand, to examine the disease progression, longitudinal deformation patterns over time need to be investigated. It calls for an effective algorithm to carry out both the shape analysis and deformation analysis of medical images. Shape and deformation analysis can both be formulated as studying the mapping between two corresponding shapes. In shape analysis, a geometric shape with a given topology can be considered a deformed shape from a template. Shape analysis and classification amongst a collection of geometric structures can then be carried out by investigating their deformation patterns from the common template. Besides, longitudinal deformation analysis can be done by studying the registration maps between images at multiple points in time. Thus, the analysis of deformation patterns plays an important role.

In the practical scenario, the deformation pattern within a certain class may not be deterministic but follow a probability distribution. For instance, the longitudinal deformation of the anatomical structures amongst the diseased group can have more than one pattern. This adds an extra challenge in deformation analysis. An effective model that allows the analysis of the probability distribution of deformations, given the data information with uncertainty, is necessary.

To address this problem, we propose to parameterize the space of deformations using computational quasiconformal (CQC) theories. More specifically, every homeomorphic deformation can be represented by its associated *Beltrami coefficient (BC)* [1, 2]. The BC captures the geometric information of the corresponding deformation. It measures the local geometric distortion (specifically the *quasiconformality*) under the deformation. Also, there is a one-to-one correspondence between the space of BCs and the space of deformations. Hence, the BC is an effective representation of the deformation. The BC can be easily computed, which obeys a partial differential equation, called the *Beltrami's equation*. With the BC, a feature vector, called the *QC feature*, given by the Fourier coefficients of the BC can be obtained. The QC feature describes the deformation and can be applied for the purpose of deformation analysis. The space of QC features inherits a simple and natural metric, namely the Frobenius distance, which makes it feasible to incorporate existing classification models for shape and deformation classification. With this framework, we propose in this paper three algorithms to handle the following tasks:

1. Develop a classification model to classify shapes with multiple modes (shape patterns) in each group;
2. Develop a classification model to classify longitudinal deformation patterns with multiple modes in each class;
3. Train a machine that can classify a new input shape into its associated class and predict its deformation, given a dataset with both the shape and longitudinal deformation pattern information.

We test our proposed algorithms on both synthetic and real medical images. Results demonstrate the efficacy of our proposed framework.

Corresponding author.

2. RELATED WORK

Shape and deformation analysis have been studied previously. For 2D shape analysis, intuitive geometric features, such as area, circularity, curvature, heat kernel and their combination, have been utilized to compare shapes [3, 4, 5, 6]. Some other contour-based shape analysis models pay more attention to local boundary information and break a contour shape into several pieces [7, 8]. Related works using conformal and quasiconformal theories for 2D shape analysis have also been proposed [9, 10, 11]. 3D shape analysis using quasiconformal theories have also been explored [12, 13, 14, 15, 16, 17]. Besides, different models have been proposed for deformation analysis. Quasiconformal models have been proposed for multiscale analysis of deformations [18] and decomposition of deformations into normal and abnormal components [19]. Besides, some models have been recently proposed to study non-deterministic deformation patterns [20, 21].

3. METHOD

In this section, we describe our proposed framework in details. We consider a collection of images $\{I_j\}_{j=1}^N$ capturing the geometric structures of interest. Associated deformations of the image domain D are used to study the geometry of shapes and their longitudinal deformation patterns.

3.1. Beltrami coefficient and Beltrami feature

Every homeomomorphic deformation $f : D \rightarrow D$ satisfies the *Beltrami's equation*:

$$\frac{\partial f}{\partial \bar{z}} = \mu(z) \frac{\partial f}{\partial z} \text{ in } D, \quad (1)$$

where $\mu = \rho + i\tau : D \rightarrow \mathbb{C}$ is called the *Beltrami coefficient (BC)* with supreme norm $\|\mu\|_\infty < 1$. The BC measures the local geometric distortion, or more specifically the quasiconformality, under f (see Figure 1)[1, 2]. Given f , its associated BC can be easily computed by the quotient of the first derivatives, according to the Beltrami's equation (1). Conversely, given μ , its corresponding deformation map can be determined. Hence, the BC is an effective representation for the deformation map. The Beltrami's equation can be reformulated as an elliptic PDE: $\nabla \cdot (A(\mu)\nabla f) = 0$, where $A(\mu) = \frac{1}{1-|\mu(z)|^2} \begin{pmatrix} (\rho-1)^2 + \tau^2 & -2\tau \\ -2\tau & (1+\rho)^2 + \tau^2 \end{pmatrix}$ is a spatial dependent matrix. Given a deformation pattern with randomness, one can describe it by considering the BC as a random field $\mu(z, \omega)$, where $\omega \in \Omega$ is the random outcome. The deformation pattern can then be regarded as the solution of the stochastic PDE: $\mathcal{L}(z, \omega)f(z, \omega) = 0$.

In the discrete case, D is a rectangular and regular mesh with $N \times N$ vertices. The BC μ is then a $N \times N$ complex

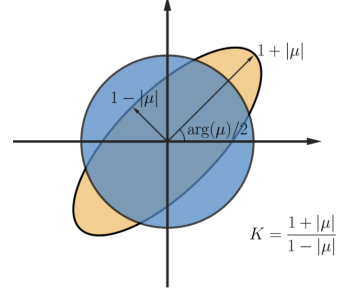


Fig. 1: Quasiconformality illustration

matrix, which can be written in terms of discrete Fourier expansion:

$$\mu(z) = \sum_{m=0}^{N-1} \sum_{n=0}^{N-1} c_{m,n} \phi_{m,n}(z), \quad (2)$$

where $\phi_{m,n} = e^{2i\frac{mx+ny}{N^2}}$ and $c_{m,n}$'s are the discrete Fourier coefficients of μ . $c_{m,n}$'s can be computed easily by fast Fourier transform (FFT).

Let $\{c_{m_k, n_l}\}_{0 \leq k, l \leq K-1}$ be Fourier coefficients associated to the lowest K^2 frequencies. Its associated BC $\tilde{\mu} = \sum_{k=0}^{K-1} \sum_{l=0}^{K-1} c_{m_k, n_l} \phi_{m_k, n_l}(z)$ corresponds to a deformation map \tilde{f} capturing the general pattern of f . We define the *QC feature* as $\mathcal{Q}_f^K = (c_{m_k, n_l})_{0 \leq k, l \leq K-1}$, which is the key ingredient for deformation analysis in this work. The whole pipeline is illustrated in Figure 2.

With the QC feature, we now describe three algorithms for shape and longitudinal deformation analysis in the following subsections.

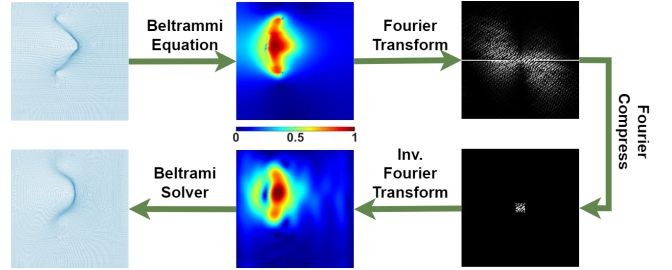


Fig. 2: QC feature computation pipeline

3.2. Shape classification model

Given a collection of images $\mathcal{S} = \{I_j\}_{j=1}^N$ capturing the geometric structures. The images I_j 's are registered to a common template image J by the registration map $f_j : D \rightarrow D$. If the topology of the geometric structure is known, the template image can be chosen as a binary image containing a simple shape (such as a circle) of the same topology (see Figure 2). If medical images are considered, an image containing the mean shape within a class can be used. Each geometric structure in I_j is then associated with a QC feature $\mathcal{Q}_{f_j}^K$. \mathcal{S} can be classified into several groups. Within each group, there can be multiple patterns or modes. Using our framework, $\{\mathcal{Q}_{f_j}^K\}_{j=1}^N$

is a distribution in K^2 -dimensional Euclidean space, which can effectively describe the probability distribution of shapes of \mathcal{S} . $\{(\mathcal{Q}_{f_j}^K, l_j)\}_{j=1}^N$, where l_j is the label representing the class of I_j , can be incorporated into conventional classification model for shape classification. In this work, we apply two approaches: 1. k -nearest neighborhood (KNN) classification and 2. deep neural network (DNN) classification. KNN classifier labels a new input data by taking into consideration of k -nearest neighbor points from the labeled training data based on the given distance. We use the simple Frobenius norm as the distance between two QC features. We then analyze the category of those neighbors and assign the category for the test data based on the majority vote. As for the DNN classification, a deep neural network (DNN) is trained, which takes the QC feature as input and outputs a vector of size is the number of classes M . The j -th entry is close to 1 if the input data belongs to class j .

3.3. Longitudinal deformation classification

Given a collection of data with longitudinal deformation information. Each data point is denoted by (I_j^1, I_j^2) , where I_j^1 and I_j^2 are images capturing the geometric structure of interest at time 1 and 2 respectively. Let $f_j : D \rightarrow D$ be the registration map between I_j^1 and I_j^2 . Suppose $\phi_j : D \rightarrow D$ parameterize I_j to a common template image J . This normalizes the geometric structure according to the template. We consider the deformation map of the template image given by $g_j = \phi_j \circ f_j \phi_j^{-1}$. Each g_j can be described by its associated QC feature $\mathcal{Q}_{g_j}^K$. Thus, the collection $\{\mathcal{Q}_{g_j}^K\}_{j=1}^N$ captures the probability distribution of the longitudinal deformation pattern. Each class can have more than one mode or deformation pattern. We apply the KNN and DNN models on $\{(\mathcal{Q}_{g_j}^K, l_j)\}_{j=1}^N$ to classify longitudinal deformation.

3.4. Joint shape classification and deformation prediction

Given a dataset with both the shape and longitudinal deformation information, our goal is to train a machine that can classify a new input shape to its associated class and predict its deformation. Each data point has two images I_j^1 and I_j^2 capturing the geometric structure at two different times and the label l_j representing the class of I_j^1 is known. As in Section 3.2, the shape of the structure in I_j^1 can be described by the QC feature $\mathcal{Q}_{f_j}^K$, where f_j is the deformation map from the template shape image to I_j^1 . According to Section 3.3, the longitudinal deformation of I_j^1 can be represented by g_j or its associated BC ν_j , where g_j is the deformation map between the template shape image. The deformation pattern can be described by $\{\mathcal{Q}_{g_j}^K\}_{j=1}^N$. As in Section 3.2, we train a classifier \mathcal{N} to classify $\{I_j^1\}_{j=1}^N$ into their corresponding classes. Thus, given a new input data I^* , we can determine its associated class by: $j_* = \mathcal{N}(I^*)$.

Next, to predict the deformation pattern of I_* , we carry out the following procedure. First, we identify the M nearest neighbor $\{\mathcal{Q}_{f_{j_m}}^K\}_{m=1}^M$ in its class according to the Frobenius norm of the QC features. Each $\mathcal{Q}_{f_{j_m}}^K$ is associated to a BC ν_{j_m} or a QC feature $\mathcal{Q}_{g_{j_m}}^K$, which describe the longitudinal deformation. Let $d_m = \|\mathcal{Q}_{f_{j_m}}^K - \mathcal{Q}_{f_*}^K\|_F^2$, where f_* is the registration map from the template to I_* and $\|\cdot\|_F$ represents the Frobenius norm. A new BC can be estimated as follows:

$$\nu_* = \sum_{m=1}^M \left(\frac{d_m}{\sum_n d_n} \right) \nu_{j_m}. \quad (3)$$

The associated deformation map g_* of ν_* can be constructed by solving Equation (1). g_* predicts the longitudinal deformation of I_* .

4. EXPERIMENTS

In this section, we test our proposed methods in Section 3 on both synthetic and real medical images. The data generation and KNN classification models are implemented by Matlab 2021a, whereas the DNN model is implemented by Python 3.6 on a Windows 11 PC with 3.20 GHz AMD Ryzen 7 5800H with Radeon Graphics. For classification, 1000 data pairs will be used, among which 800 are used for training and 200 for testing. The resolution of the input image is uniform 256×256 . We set $K = 10$ for the QC features.

Method	Ana. Shape	Brain Shape	Brain Deform.
KNN	99.99	83.18	80.76
DNN	99.99	93.24	92.96

Table 1: Classification accuracy

4.1. Synthetic and Brain Shape Classification

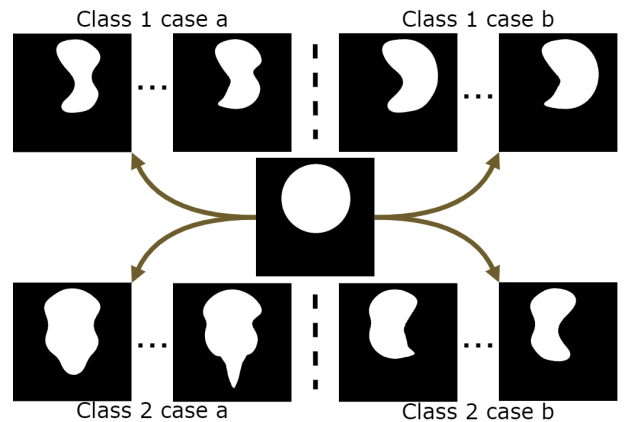


Fig. 3: Synthetic experimental results

We first test the shape classification model proposed in Section 3.2. Figure 3 shows a synthetic example. Shapes

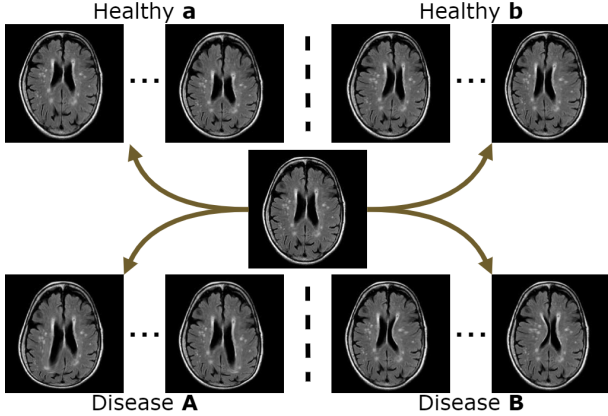


Fig. 4: Shape analysis results on medical images

are labeled into classes, of which there are two shape patterns or modes in each class. The QC features for each shapes are computed. Using *multidimensional scaling (MDS)*, we can visualize the distribution of the QC features according to their Euclidean distances, which is as shown in Figure 5(a). We applied both the KNN and DNN models for shape classification. Both methods performed very well with 99.99% accuracy as reported in Table 1. Figure 4 shows a collection of brain MRIs with different shapes of the lateral ventricles. The collection is partitioned into two groups. One groups contains images whose lateral ventricles are believed to be normal. The other group contains images whose lateral ventricles are abnormally deformed. Abnormal shapes of lateral ventricles are often observed amongst patient suffering brain injuries, such as Periventricular Leukomalacia. Each group contains two shape modes. As shown in Figure 5(b), *Healthy a* are close to *Diseased A* in distance, although they are considered to be totally different group. Such a subtle difference in Euclidean distance resulted in 83.18% classification accuracy for KNN model. It is notably lower than that by the DNN model, which achieves 93.24%.

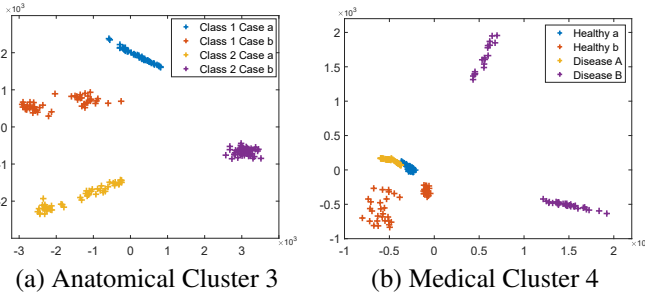


Fig. 5: Plots of QC features by MDS

4.2. Longitudinal Shape Classification

We also test our model for longitudinal deformation analysis. Figure 6 shows the longitudinal deformations of lateral ventricles in some brain MRIs. In this experiments, we have a collection of 1000 deformations, which are classified into two groups. Each group contains two deformation patterns.

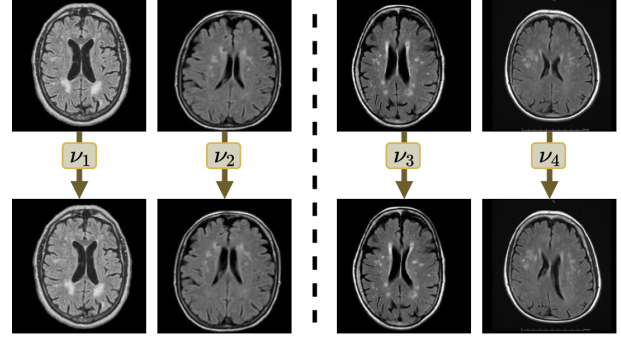


Fig. 6: Longitudinal deformation analysis on medical images

800 of them are used as training data and 200 are used as the testing data. As reported in Table 1, the classification accuracy of the KNN classifier is 80.76%. The DNN classifier can achieve a much higher accuracy, which is 92.96%.

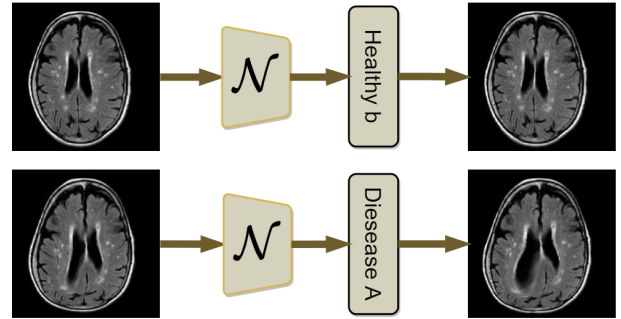


Fig. 7: Illustration of joint shape classification and deformation prediction model

4.3. Joint shape classification and deformation prediction

The diagnosis of disease and the prediction of the disease progression are two important tasks in medical image analysis. These tasks can be simultaneously achieved using our model, as described in Section 3.4. Figure 7 demonstrates the results using our proposed model. The top brain MRI is classified as a normal subject and the predicted deformation of the lateral ventricle is subtle. The bottom brain MRI is classified to contain an abnormal lateral ventricle, whose predicted deformation is more severe without proper medical intervention.

5. CONCLUSION

In this paper, we address the problem of analyzing the shape and deformation pattern of geometric structures. We formulate the problem in terms of deformation analysis. We propose to apply the QC feature based on quasiconformal theories to describe the deformation pattern. The collection of QC features captures the distribution of deformations as data points in a high-dimensional Euclidean space. Using the framework, we develop models for shape classification, longitudinal deformation classification and joint shape classification and deformation prediction.

6. REFERENCES

- [1] Frederick P Gardiner and Nikola Lakic, *Quasiconformal teichmuller theory*, Number 76. American Mathematical Soc., 2000.
- [2] Lok Ming Lui, Ka Chun Lam, Tsz Wai Wong, and Xianfeng Gu, “Texture map and video compression using beltrami representation,” *SIAM Journal on Imaging Sciences*, vol. 6, no. 4, pp. 1880–1902, 2013.
- [3] Markus Peura, Jukka Iivarinen, et al., “Efficiency of simple shape descriptors,” in *Proceedings of the third international workshop on visual form*, 1997, vol. 5, pp. 443–451.
- [4] Serge Belongie, Jitendra Malik, and Jan Puzicha, “Shape matching and object recognition using shape contexts,” *IEEE Trans. Pattern Analysis & Machine Intelligence*, vol. 24, no. 4, pp. 509–522, 2002.
- [5] Haruo Asada and Michael Brady, “The curvature primal sketch,” *IEEE Trans. Pattern Analysis & Machine Intelligence*, , no. 1, pp. 2–14, 1986.
- [6] Jian Sun, Maks Ovsjanikov, and Leonidas Guibas, “A concise and provably informative multi-scale signature based on heat diffusion,” in *Computer Graphics Forum*. Wiley Online Library, 2009, vol. 28, pp. 1383–1392.
- [7] William I Grosky and Rajiv Mehrotra, “Index-based object recognition in pictorial data management,” *Computer vision, Graphics, and Image processing*, vol. 52, no. 3, pp. 416–436, 1990.
- [8] Stefano Berretti, Alberto Del Bimbo, and Pietro Pala, “Retrieval by shape similarity with perceptual distance and effective indexing,” *IEEE Trans. on Multimedia*, vol. 2, no. 4, pp. 225–239, 2000.
- [9] Eitan Sharon and David Mumford, “2d-shape analysis using conformal mapping,” *Int. J. of Computer Vision*, vol. 70, no. 1, pp. 55–75, 2006.
- [10] Lok Ming Lui, Wei Zeng, Shing-Tung Yau, and Xianfeng Gu, “Shape analysis of planar multiply-connected objects using conformal welding,” *IEEE Trans. Pattern Analysis & Machine Intelligence*, vol. 36, no. 7, pp. 1384–1401, 2013.
- [11] Chenran Lin and Lok Ming Lui, “Harmonic beltrami signature: A novel 2d shape representation for object classification,” *arXiv preprint arXiv:2103.16411*, 2021.
- [12] Wei Zeng, Lok Ming Lui, Lin Shi, Defeng Wang, Winnie CW Chu, Jack CY Cheng, Jing Hua, Shing-Tung Yau, and Xianfeng Gu, “Shape analysis of vestibular systems in adolescent idiopathic scoliosis using geodesic spectra,” in *Proc. of Int. Conf. on Medical Image Computing and Computer-Assisted Intervention*. Springer, 2010, pp. 538–546.
- [13] Lok Ming Lui, Tsz Wai Wong, Wei Zeng, Xianfeng Gu, Paul M Thompson, Tony F Chan, and Shing Tung Yau, “Detection of shape deformities using yamabe flow and beltrami coefficients,” *Inverse Problems & Imaging*, vol. 4, no. 2, pp. 311, 2010.
- [14] Hei Long Chan, Hangfan Li, and Lok Ming Lui, “Quasi-conformal statistical shape analysis of hippocampal surfaces for alzheimer’s disease analysis,” *Neurocomputing*, vol. 175, pp. 177–187, 2016.
- [15] Gary PT Choi, Hei Long Chan, Robin Yong, Sarbin Ranjitkar, Alan Brook, Grant Townsend, Ke Chen, and Lok Ming Lui, “Tooth morphometry using quasi-conformal theory,” *Pattern Recognition*, vol. 99, pp. 107064, 2020.
- [16] Miao Jin, Wei Zeng, Feng Luo, and Xianfeng Gu, “Computing teichmuller shape space,” *IEEE Trans. Visualization & Computer Graphics*, vol. 15, no. 3, pp. 504–517, 2009.
- [17] Zhengyu Su, Yalin Wang, Rui Shi, Wei Zeng, Jian Sun, Feng Luo, and Xianfeng Gu, “Optimal mass transport for shape matching and comparison,” *IEEE Trans. Pattern Analysis & Machine Intelligence*, vol. 37, no. 11, pp. 2246–2259, 2015.
- [18] Ka Chun Lam, Tsz Ching Ng, and Lok Ming Lui, “Multiscale representation of deformation via beltrami coefficients,” *Multiscale Modeling & Simulation*, vol. 15, no. 2, pp. 864–891, 2017.
- [19] Ho Law, Chun Yin Siu, and Lok Ming Lui, “Decomposition of longitudinal deformations via beltrami descriptors,” *Journal of Scientific Computing*, vol. 89, no. 1, pp. 1–28, 2021.
- [20] Qian Ge, Namita Lokare, and Edgar Lobaton, “Non-rigid image registration under non-deterministic deformation bounds,” in *International Symposium on Medical Information Processing and Analysis*. International Society for Optics and Photonics, 2015, vol. 9287, p. 92870T.
- [21] Alexis Arnaudon, Darryl D Holm, Akshay Pai, and Stefan Sommer, “A stochastic large deformation model for computational anatomy,” in *Int. Conf. on Information Processing in Medical Imaging*. Springer, 2017, pp. 571–582.